First Results of Dutch Peatland Subsidence Observations Using InSAR

P. Conroy*, S.A.N. van Diepen, F.J. van Leijen, R.F. Hanssen

1 Department of Geoscience and Remote Sensing, Delft University of Technology

p.n.conroy@tudelft.nl

Introduction

Land subsidence in the Netherlands is becoming an increasingly critical issue as it is closely linked with sea level rise, flooding risks and greenhouse gas emissions due to peat oxidation (Erkens et al., 2016; Erkens et al., 2016). Despite the importance of this issue, it is very difficult to accurately assess subsidence levels across the country. SAR Interferometry (InSAR) is a very promising technique for monitoring land surface motion at large spatial scales with frequent temporal sampling. While InSAR techniques employing stable point scatterers (PS) have been successfully used to monitor subsidence in the Netherlands (Caro Cuenca & Hanssen, 2008; Caro Cuenca et al., 2011; Hanssen et al., 2018), these PS points are usually founded at greater depths and the movement of the surrounding landscape has had to be indirectly inferred.

So far, it has been impossible to directly observe land surface motion using distributed scatterer (DS) techniques in the Netherlands because rapid soil movement, seasonal land use changes and high noise levels result in sudden losses of interferometric coherence, rendering any such attempt extremely challenging (Morishita & Hanssen, 2015; Heuff & Hanssen, 2020).

We present a first test of a novel methodology for InSAR processing which makes use of contextual data and machine learning techniques to robustly estimate a surface motion time series using C-band Sentinel-1 InSAR at the parcel scale. To our knowledge, this is the first accurate InSAR time series of a Dutch grassland polder region.

Methods

Contextual Data Integration

We assemble a database of combined public cadastral parcel delineations and land cover data, soil maps, and groundwater management zones, available: PDOK. These factors play a critical role in either the movement of the land surface, the scattering properties which affect the radar observation, or both. By cross-referencing this data with the SAR imagery, we can assign each pixel to a known parcel ID with known soil, land use and land cover (LULC), and groundwater parameters. This ensures that we are processing homogeneous observations which are representative of the same land surface movement phenomena.

Parcel Multilooking and Phase Estimation

After the dataset of contextual data is prepared, we multilook the native 5×20 meter Sentinel-1 observations according to the parcel delineations of the contextual dataset. This is a natural division to make, as the land cover, soil type, and groundwater are approximately consistent within a parcel. This also ensures a high multilooking degree of approximately 100 equivalent looks (although this varies with each parcel according to its shape and size) which aids in suppressing noise (Hanssen,

2001). Following the multilooking step, we perform phase estimation using the EMI method (Ansari et al., 2018).

Segmentation and Temporal Phase Ambiguity Resolution

Rapidly changing displacement phases and noise make the application of standard phase unwrapping algorithms very unreliable, and often large movements in one direction are misinterpreted as smaller movements in the opposite direction (Alshammari et al., 2018; Tampuu et al., 2022). This motivated the development of a machine-learning aided phase unwrapping algorithm, described in Conroy et al (2022). The algorithm uses rainfall and temperature data to anticipate large subsidence and uplift events in order to guide phase ambiguity resolution in the temporal domain.

The second major hurdle preventing successful InSAR estimations are the sudden losses of coherence in the time series. Especially during the (late) summer period, coherence levels can often drop to such low levels that there is essentially no useful information retained in the interferograms with even the shortest temporal baseline (6 days). Whenever this occurs, we designate the event as a "Loss-of-Lock" and divide the time series into separate segments. While we can unwrap each individual temporal segment with a satisfactory degree of reliability, the segments themselves are disconnected, and an unknown vertical shift exists between segment (Conroy et al., 2022). We can reconnect the segments by observing neighbouring parcels. While each parcel follows a similar general pattern, the actual date during which coherence drops below the useable threshold is different in each case. Thus by using contextual information to group similar parcels together, we can use the aggregate of all segments in a group to fully span the incoherent periods with coherent observations.

This is accomplished by fitting a kinematic model to the unwrapped segments. For this purpose, we use a simple seasonal plus linear (SL) model, which can be used to approximately estimate the mean position of a segment without making many assumptions. The total number of segments in a group is N = (Num. SAR tracks) × (Num. parcels per group) × (Num. segments per parcel). The SL model is parameterized by the vector θ, and given N segments, there are N + 3 parameters to estimate:

$$
\boldsymbol{f_g}(\boldsymbol{\theta}, t) = \begin{cases} \theta_1 \cos(2\pi f_a t + \theta_2) + \theta_3 t + \theta_4, & \text{for } i = 1 \\ \theta_1 \cos(2\pi f_a t + \theta_2) + \theta_3 t + \theta_5, & \text{for } i = 2 \\ \quad\quad\quad\vdots \\ \theta_1 \cos(2\pi f_a t + \theta_2) + \theta_3 t + \theta_{N+3}, & \text{for } i = N \end{cases} \tag{1}
$$

where t is the independent variable representing time, and fa denotes an annual frequency. The vector θ contains all the estimated parameters of the displacement model: θ1 is the amplitude of the annual periodic component, θ2 is the phase offset of the annual periodic component, θ3 is the linear rate and θi+3 is the estimated vertical shift of the ith segment. Note that the parameters [θ1, θ2, θ3] are the same for every segment in a given group g characterized by the model fg. The model is fit by minimizing the mean squared error between the model and the segment during the coherent period.

Spatial Ambiguity Resolution

High noise levels in the individual parcels make applying a geodetic network approach to spatial ambiguity resolution very challenging (van Leijen, 2014). However, a less strict spatial ambiguity constraint is applied by considering the phase changes between consecutive interferograms of a given parcel, Δϕ, versus its corresponding group mean, Δϕ̄:

$$\Delta\phi_{new} = \begin{cases} \Delta\phi_{\text{old}} + 2\pi, & \text{for } |\Delta\phi_{\text{old}} + 2\pi - \Delta\bar{\phi}| < |\Delta\phi_{\text{old}} - \Delta\bar{\phi}| \\ \Delta\phi_{\text{old}} - 2\pi, & \text{for } |\Delta\phi_{\text{old}} - 2\pi - \Delta\bar{\phi}| < |\Delta\phi_{\text{old}} - \Delta\bar{\phi}| \\ \Delta\phi_{\text{old}}, & \text{otherwise.} \end{cases} \tag{2}$$

Each parcel is checked and the ambiguities are adapted according to equation (2). The group mean is recalculated once the spatial unwrapping procedure is completed for all parcels.
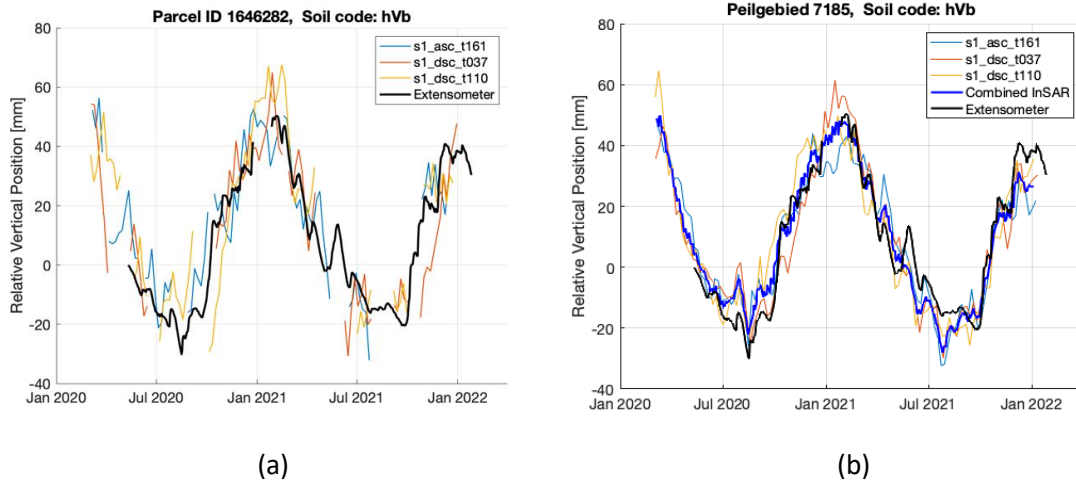
Results

(a) (b)

Figure 1 (a) Parcel example of a grassland polder where a peat soil is covered by up to 15 cm clay/peat. Three independent Sentinel-1 track results are shown relative to the reference extensometer. (b) Group time series estimations plotted against validation data obtained from the Zegveld test site.

Time Series Validation Against Ground Truth

We validate the approach described in Section 2 against in-situ measurements taken by an extensometer, which provides hourly measurements of Holocene soil displacement at a given location (van Asselen et al., 2020). A 10x10 km study area surrounding Zegveld, the Netherlands is observed between Apr. 1, 2020 and Jan. 15, 2022. These dates are chosen as they correspond with the installation of an Integrated Geodetic Reference Station (IGRS) with corner reflectors which is used as the reference point, and the failure of the Sentinel-1b satellite in early 2022, respectively.

Two types of output are available: partial time series estimations per parcel (shown in Figure 1a) and full time series estimations per group (Figure 1b). It should be noted that while the extensometer provides measurements at one point, the InSAR time series is a spatial average of many points, and will therefore differ from the extensometer as some short term variations are filtered out of the result. Note that this spatial filtering effect will be stronger for the group result. The validation parcel belongs to a larger group of 51 parcels, which, based on the contextual data available, we expect to behave in a broadly similar fashion. A wholly continuous time series of the group can be estimated by taking the median of all time series segments. This has the benefit of strongly reducing the effects of noise and phase unwrapping errors at the cost of reduced spatial resolution.

Initial Spatial Results

A spatial plot showing the estimated linear deformation rate per parcel is shown in Figure 2. The time series used in this study is too short to provide accurate estimates of linear irreversible subsidence rates, however, we can assess both the spatial correlation of the result and compare the order of magnitude to the expected level.
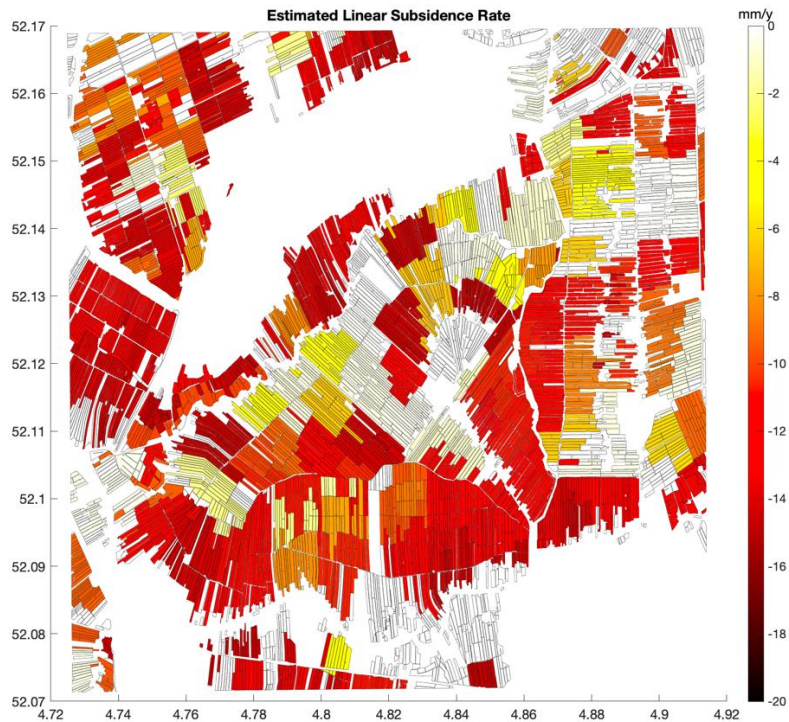
Figure 2   Zegveld linear displacement rate map. Uncoloured parcels indicate that no estimation is made at that location.

Conclusion

We demonstrate a new methodology for estimating the ground motion of cultivated peatlands using DS time series InSAR. Our initial results show that the approach is promising, and we have been able to successfully validate our result against the ground truth data we have available. To our knowledge this is first accurate InSAR measurement of peatland surface motion in the Netherlands. Following this successful test, we plan to process a longer time series in order to obtain more accurate long-term subsidence estimates and to allow for comparison between seasons as a response to climatic stimuli.

Acknowledgement

References

Erkens, G., van der Meulen, M. J., Middelkoop, H. (2016). "Double trouble: Subsidence and CO2 respiration due to 1,000 years of Dutch coastal peatlands cultivation," *Hydrogeology Journal*, vol. 24, no. 3, pp. 551–568

Erkens, G., Bucx, T., Dam, Lange, R. D., Lambert, J.G. (2016). Sinking Cities: An Integrated Approach to Solutions, In: The Making of a Riskier Future: How Our Decisions Are Shaping Future Disaster Risk. *World Bank*.

Caro Cuenca, M., Hanssen, R. F. (2008). "Subsidence due to peat decomposition in the Netherlands, kinematic observations from radar interferometry," in Proc. *ESA Fringe Workshop*, (Frascati, Italy), pp. 1–6.

Caro Cuenca, M., Hanssen, R. F., Hooper, A., Arikan, M. (2011). "Surface deformation of the whole Netherlands after PSI analysis," in Proc. *ESA Fringe Workshop*, (Frascati, Italy), pp. 19–23.

Hanssen, R. F., Van Leijen, F. J., Erkens, G., Stouthamer, E., Cohen, K., Lange, Meulen, Akker and Others (2018). *"Land motion service of the Netherlands*,".

Morishita, Y., Hanssen, R. F. (2015). "Deformation parameter estimation in low coherence areas using a multisatellite InSAR approach," *IEEE Transactions on Geoscience and Remote Sensing*, vol. 53, no. 8, pp. 4275–4283.

Heuff, F. M., Hanssen, R. F. (2020). "InSAR phase reduction using the remove-compute-restore method," in 2020 *IEEE International Geoscience and Remote Sensing Symposium*, pp. 786–789.

"Publieke Dienstverlening Op de Kaart (PDOK*)." www.pdok.nl.*

Hanssen, R. F. (2001). *Radar Interferometry: Data Interpretation and Error Analysis*. Dordrecht: Kluwer Academic Publishers.

Ansari, H., De Zan, F., Bamler, R. (2018). "Efficient phase estimation for interferogram stacks," *IEEE Transactions on Geoscience and Remote Sensing*, vol. 56, no. 7, pp. 4109–4125.

Alshammari, L., Large, D. J., Boyd, D. S., Sowter, A., Anderson, R., Andersen, R., Marsh, S. (2018). "Long-term peatland condition assessment via surface motion monitoring using the ISBAS DInSAR technique over the flow country, Scotland," Remote Sensing, vol. 10, no. 7.

Tampuu, T., De Zan, F., Shau, R., Praks, J., Kohv, M., Kull, A. (2022). "Reliability of sentinel-1 InSAR distributed scatterer (DS) time series to estimate the temporal vertical movement of ombrotrophic bog surface," *in EGU General Assembly*, vol. EGU22-2387, (Vienna, Austria).

Conroy, P., Van Diepen, S. A. N., Van Asselen, S., Erkens, G, Van Leijen, F. J., Hanssen, R. F. (2022). "Probabilistic estimation of InSAR displacement phase guided by contextual information and artificial intelligence," *IEEE Transactions on Geoscience and Remote Sensing*, vol. 60, pp. 1–11.

Conroy, P., Van Diepen, S. A. N., Van Leijen, F. J., Hanssen, R. F. (2022) "Hybrid InSAR processing for rapidly deforming peatlands aided by contextual information," *in 2022 IEEE International Geoscience and Remote Sensing Symposium*.

Van Leijen, F. (2014). Persistent Scatterer Interferometry based on geodetic estimation theory. *PhD thesis*, TU Delft.

Van Asselen, S., Erkens, G., De Graaf, F., (2020). "Monitoring shallow subsidence in cultivated peatlands," *Proceedings of the International Association of Hydrological Sciences*, vol. 382, pp. 189–194.